Desalination and Water Treatment
www.deswater.com
doi: 10.1080/19443994.2015.1049958

57 (2016) 12536–12545
June

Taylor & Francis
Taylor & Francis Group

Magnetic pomelo peel as a new absorption material for oil-polluted water

Junchen Zou, Wenbo Chai, Xiaoyan Liu*, Beibei Li, Xinying Zhang, Tiantian Yin

College of Environmental and Chemical Engineering, Shanghai University, 99 Shangda Road, Shanghai 200444, P.R. China, Tel. +15036065609; email: Junchen526@163.com (J. Zou), Tel. +18818215695; email: 526203314@qq.com (W. Chai), Tel. +862166137767; email: lxy999@shu.edu.cn (X. Liu), Tel. +18818216331; email: 743421914@qq.com (B. Li), Tel. +18917802319; email: 864354276@qq.com (X. Zhang), Tel. +18101032207; email: 249359327@qq.com (T. Yin)

Received 13 August 2014; Accepted 5 May 2015

ABSTRACT

Magnetic pomelo peel (MPP) with high oil sorption capacity was prepared by solvothermal method. The characteristics of MPP were manifested by FTIR, SEM, XRD, and vibrating sample magnetometry. Adsorption kinetics and equilibrium of diesel from aqueous solution on MPP were studied in a batch process. The kinetic studies showed good correlation coefficients for the pseudo-second-order kinetic model, and the equilibrium process was well described by the Freundlich isotherm model. The maximum sorption capacity of MPP was 27.98 g/g for diesel at 30°C. The results in this study indicated that MPP was an attractive candidate for removing oil from aqueous solutions.

Keywords: Pomelo peel; Magnetic material; Oil spill; Sorption

1. Introduction

With the extensive transportation and application of oil, oil spill occurs frequently worldwide. When oil spill occurs at sea, a mass of physical, chemical, and biological processes takes place simultaneously, including spreading, evaporation, emulsion, oxidation, and bioremediation [1]. Such accidents can cause severe pollution of coastal waters (e.g. the Gulf of Mexico oil spill accident in 2010) and human living environment and they can also lead to a significant loss of valuable resources [2,3]. Therefore, it is vital and necessary to develop a technology to recover the spilled oil.

The possibility of making use of magnetic materials to recover the spilled oil has been considered since 1973 [4,5], such as magnetic adsorbents based on activated carbon/iron oxide [6], bentonite/iron oxide composites [7]. These magnetic composites not only combined the excellent adsorption features of bentonite and activated carbon, but also could be able to remove contaminants from aqueous solution with the magnetic properties of iron [8,9]. Some researchers found that super-hydrophobic and super-oleophilic magnetic spheres could be placed on the surface of the polluted water and subsequently be removed by means of an external magnetic field [10–13].

Pomelo peel (PP) was disposed at random and caused severe problem in the community. Zhou et al. [14] found that PP had homogeneous macropore size which centered at approximately 2–20 μm. Some literatures had reported that PP had been used as a sorbent to remove basic dye from aqueous solution [15]. In order to make PP easier to control and recover the spilled oil, magnetic pomelo peel (MPP) was studied. Thus, when a magnetic field was set up around the

*Corresponding author.

spilled oil area, MPP adsorbed with plenty of oil could promptly be collected.

2. Materials and methods

2.1. Materials

PP (the content of cellulose, hemicellulose, and lignin of PP in this study were 46.22, 18.84, and 10.24% by weight, respectively) was collected from nearby market as solid waste. The collected materials were washed with distilled water for several times to remove all the dirt particles, dried in a hot air oven at 60℃ for 48 h, and then stripped the yellow skin and crushed into granules. The fraction with sample size between 0.25 and 1.00 mm was subjected to be dried in a hot air oven at 60℃ for 48 h and then stored in air tight container for further use.

Diesel (density at 20℃ = 0.8170 g/cm^3, viscosity = 6.51 mm^2/s) was obtained from Minghe petrol station of Sinopec in Baoshan district, Shanghai; Oleic acid, $FeCl_3{\cdot}6H_2O$, Ethylene glycol, NH_4Ac, and other reagents used were of analytical grades (Sinopharm Chemical Reagent Co., Ltd).

2.2. Procedures of sample preparation

A total of 0.4 g $FeCl_3{\cdot}6H_2O$ was dissolved in 30 mL of ethylene glycol to form a clear solution, followed by the addition of NH_4Ac (3.4 g), PP (0.2 g), and oleic acid (0.4 mL). The mixture was stirred vigorously for 30 min and then sealed in a teflon-lined stainless steel autoclave (50 mL). The autoclave was heated to 200℃ and maintained at 200℃ for 6 h, and allowed to cool to room temperature. The black products were washed several times with ethanol and dried at 60℃ for 6 h. The magnetic PP was denoted as MPP, whereas for specific comparison purpose, PP heated at 200℃ for 6 h without any reagent was denoted as carbonized pomelo peel (CPP).

2.3. Characterization

FTIR: Infrared spectrum of MPP and CPP was analyzed using an FTIR (Nicolet 380). A total of 2 mg sample was mixed with 200 mg of KBr and then compressed into a pellet. FTIR of the samples were obtained at the range of 4,000–400 cm^{-1}.

SEM: MPP morphology was analyzed by scanning electron microscopy (SEM, SU-1510). For SEM analysis, the samples were mounted on round stainless steel sample holders with double-sided conductive adhesive tapes. The samples were sputter-coated with gold to provide conductive coating that enhanced the images under SEM. SEM images were examined using accelerating voltage at 15 kV.

XRD: The diffraction patterns of the samples studied were recorded by DLMAX-2200 diffractometer, which was operated at 40 kV and 250 mA. The XRD patterns were recorded in the 2θ range 5–60˚ at 0.02 steps. The samples for the experiments were powdered and pressed into a sample holder. Samples with the radius of 1 cm and the thickness of 0.6 mm thick were prepared.

VSM: Vibrating sample magnetometry (Lakeshore 7407) was performed to obtain the magnetization loop of the samples that were prepared at 300 K.

2.4. Batch kinetic studies

To the batch kinetic studies, 0.01 g of MPP was placed in a 50-mL conical flask containing 30 mL of deionized water and 1 mL of diesel maintained at 30℃ and left for 2 h with 150 rpm. Samples were withdrawn by means of an external magnetic field at different time intervals up to the equilibrium, then 0.1 mL of the slurry was extracted by 9.9 mL of n-hexane with a 125-mL separating funnel. The extracted liquid was determined with the constant volume of 10 mL and its concentration was determined using an ultraviolet spectrophotometer at a wavelength of 225 nm, using n-hexane as a reference. The concentration of the diesel oil was obtained from the following equation:

$$C_{oil} = Q\frac{V_1}{V_2} \tag{1}$$

where in C_{oil} is the concentration of the simulated diesel solution (mg/L); Q is the concentration of the extracted liquid (mg/L); V_1 is the volume of the extracted liquid (mL); and V_2 is the volume of the simulated diesel solution (mL).

The sorption capacity for diesel was obtained from the following equation:

$$Q_1 = (C_0 - C_{oil})\frac{V}{M} \tag{2}$$

where in Q_1 is the sorption capacity (g/g); C_0 is the concentration of the original diesel solution (mg/L); C_{oil} is the concentration of the diesel solution after sorption (mg/L); V is the volume of the solution (L); and M is the weight of the MPP (g).

Experiments were duplicated and the average values were used in the calculations.

2.5. Batch isotherm experiments

Batch isotherm experiments were conducted in the oil-in-water emulsions and at different temperature (20, 25, 30°C). Six representative diesel quantities (0.25, 0.5, 0.75, 1, 1.25, and 1.5 mL) were selected. Different quantities of diesel were mixed with 30 mL of deionized water and 0.01 g of MPP at 150 rpm. After the equilibrium time, all the samples were withdrawn by means of an external magnetic field, then the slurry was extracted by n-hexane and analyzed for oil in water. All the experiments were duplicated and the average values were used in the calculations.

2.6. Effect of sorbent dosage

To determine the effect of sorbent dosage, five samples weighing 0.01, 0.03, 0.05, 0.07, and 0.09 g were placed into a 150-mL glass beaker containing with 1 mL diesel and 30 mL deionized water. The beaker was maintained at 25°C for 20 min and stirred at 150 rpm. After 20 min, the sample was placed into the beaker for 1 h, then the samples were withdrawn by means of an external magnetic field.

2.7. Effect of diesel dose

Different diesel dose (0.25, 0.50, 0.75, 1.00, 1.25, and 1.50 mL) with 30 mL deionized water were prepared in a series of 150 mL beakers, and 0.01 g of MPP was placed into the beaker maintained at 20, 25, 30°C for 20 min and stirred at 150 rpm. After 20 min, the sample was placed into the beaker for 1 h and then, the samples were withdrawn by means of an external magnetic field.

2.8. Reusability

The sample (0.01 g) was placed into a 150-mL glass beaker containing with 1 mL diesel and 30 mL deionized water. The beaker was maintained at 25°C for 20 min and stirred at 150 rpm. After 20 min, the sample was placed into the beaker for 1 h, then the samples were withdrawn by means of an external magnetic field. Finally, the oil-loaded sample was transferred into a 500-mL beaker containing 300 mL n-hexane. After 10 min extracting, the sample was directly dried in a 60°C oven before use. The test was repeated and the oil sorption capacity of the sample after each cycle was evaluated.

3. Results and discussion

3.1. Characterization

To understand the adsorption mechanism of MPP, infrared spectrum is conducted for CPP and MPP. The existence of Fe–O stretching bands at 573 cm^{-1} shows magnetic nanoparticles are successfully prepared (Fig. 1). The existence of magnetite covered with oleic acid shows CH_2 stretching bands at <3,000 cm^{-1} (i.e. 2,854 and 2,924 cm^{-1}), which are attributed to the symmetric and asymmetric CH_2 stretching. Noting that the FTIR of pure liquid oleic acid show C=O stretch bands at 1,710 cm^{-1} [16]; however, the C=O stretch bands of carboxylate appear at 1,450 cm^{-1} [17–19]. These results suggest that the bonding pattern of the carboxylic acid on the surface of magnetic nanoparticles is a combination of molecules bonded symmetrically and molecules bonded at an angle to the surface [20].

Scanning electron micrographs (SEM) of CPP and MPP are shown in Fig. 2. It can be observed that CPP is blocky and has smooth surface. However, there are many smaller holes of MPP, indicates that increased specific surface area, and distributed uniformly in the surface of MPP.

The X-ray diffraction spectra of CPP and MPP are shown in Fig. 3. It can be observed that the major diffraction peaks of CPP and MPP appear in the position of 2θ close to 22.12°, where represent both crystalline and amorphous material [21]. Compared with CPP, the crystallinity of MPP is significantly declined. Some research found that the diffraction peaks of Fe_3O_4 nanoparticles were at $2\theta = 35.2°$ and 57.1°, it was consistent with the diffraction peak of MPP [22]. Moreover, the research found that the diffraction peak of oleic acid-treated Fe_3O_4 nanoparticles was consistent with the diffraction peak of pure Fe_3O_4 nanoparticles, it was proved that the crystal shape of the oleic acid-treated Fe_3O_4 nanoparticles remained the same.

It was reported that magnetic nanoparticles prepared by the coprecipitation method had many hydroxyl groups on the surface of precipitates [23].

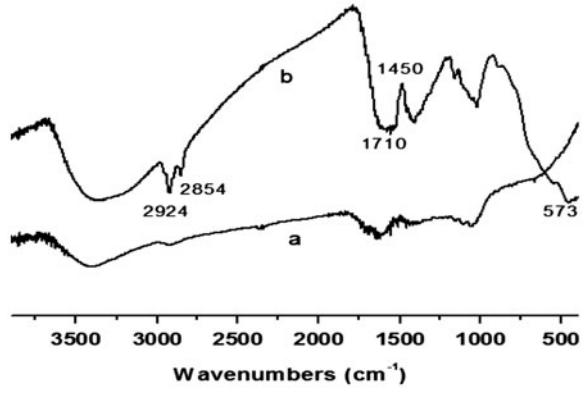

Fig. 1. FTIR spectrum of (a) carbonized pomelo peel (CPP) and (b) magnetic pomelo peel (MPP).

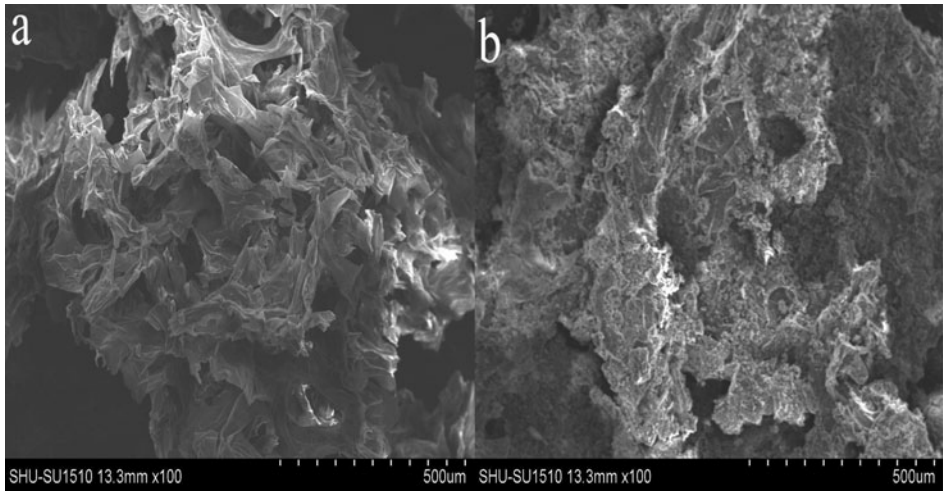

Fig. 2. SEM images of CPP (a) and MPP (b).

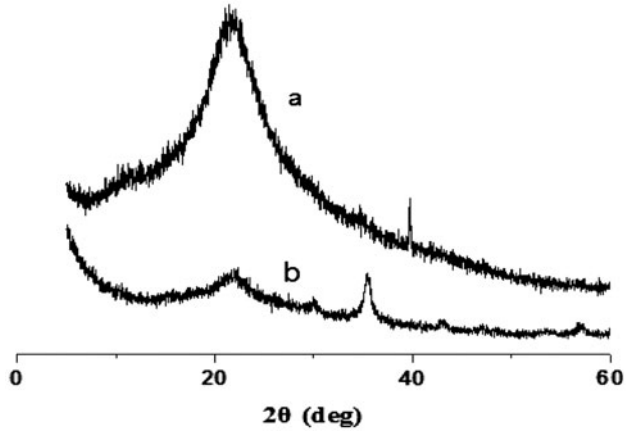

Fig. 3. XRD cures of (a) CPP and (b) MPP.

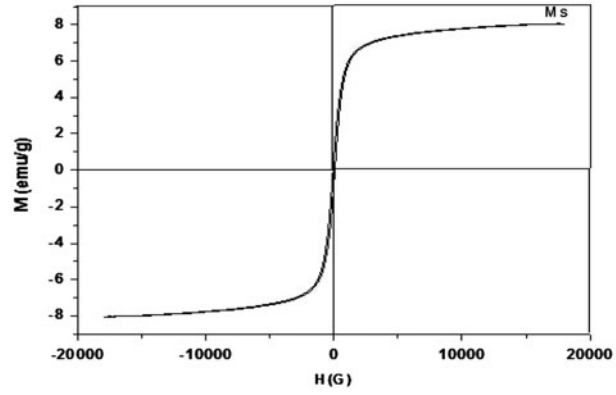

Fig. 4. Room temperature magnetization curves of MPP.

Because of dipole attraction, the uncoated magnetite particles were easy to agglomerate. To avoid this, oleic acid was coated on the surface of the particle. The magnetic properties of MPP were investigated with VSM at 300 K. Fig. 4 shows the magnetic saturation value of MPP is 8.06 emu g^{-1}, which is smaller than the magnetic saturation value of aggregate Fe_3O_4 material (90 emu g^{-1}), indicate that MPP can move in solution by means of external magnetic field. The smaller MS values could be due to an increase in the surface anisotropy induced by the chemisorption of oleic acid [24]. Inside the aggregate, the oleic acid layers separated the nanoparticles, and this distance decreased the dipolar magnetic interactions among the iron oxide nanoparticles. Furthermore, the magnetic particles remained in suspension for more than 1 d, which demonstrated that they could be well-dispersed in aqueous solution (Fig. 5).

3.2. Adsorption kinetics study

To determine relevant parameters, batch kinetic data obtained were processed in conjunction with appropriate models mentioned in the literature [25]. In this connection, both the pseudo-first-order and the pseudo-second-order adsorption kinetic models are presented in the following. The pseudo-first-order adsorption kinetics can be described as:

$$\frac{dq}{dt} = k_1(q_e - q_t) \tag{3}$$

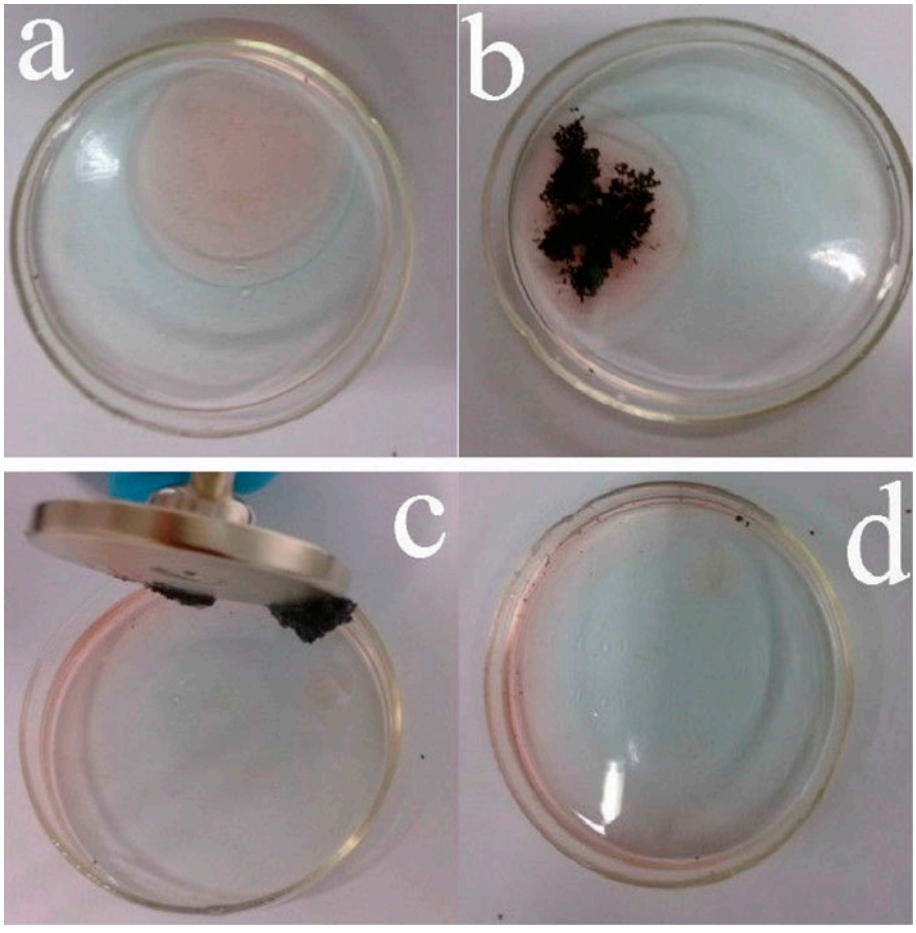

Fig. 5. The process of removing diesel on water surface with MPP. (a) Appearance of diesel floating on the water surface. (b) MPP was added. (c) MPP saturated with diesel separated by a small magnet. (d) The clean water after diesel removed by MPP.

where in q_e is the equilibrium amount of adsorbed contaminant (g) per unit mass (g) of the adsorbent, q_t is adsorbed amount at any time t, and k_1 is the first-order rate constant (1/min). Integrating the above equation with the limit $q = 0$ at time $t = 0$ gives:

$$\ln\frac{q_e - q_t}{q_e} = -k_1 t \tag{4}$$

Eq. (3) can also be rewritten as:

$$\ln(q_e - q_t) = -k_1 t + \ln q_e \tag{5}$$

It is clear from Eq. (4) that a plot of $\ln(q_e - q_t)$ vs. time yields a straight line of slope $-k_1$ and the y-intercept as $\ln(q_e)$. The experimental data and fits are shown in Figs. 6 and 7.

The agreement is not good in the case of diesel. The parameter values, i.e. the rate constant k_1 and q_e, are computed from the slope and the intercepts of the fitted curves, and reported in Table 1.

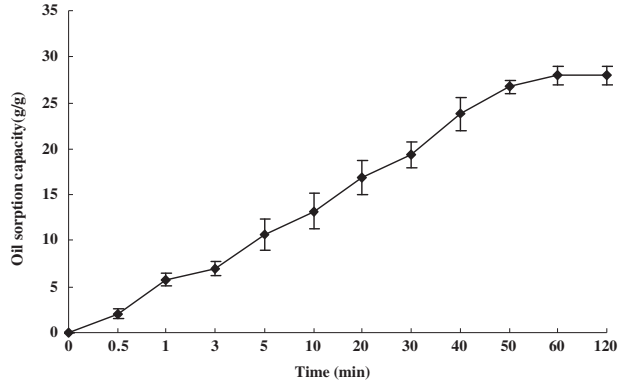

Fig. 6. Adsorption kinetic curves of MPP.

On the other hand, the pseudo-second-order adsorption kinetics is represented as:

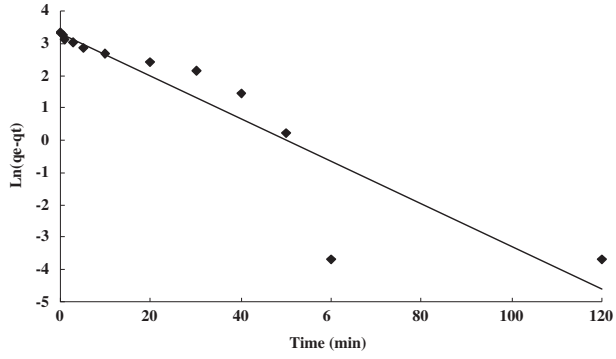

Fig. 7. Dynamic fitting results for the pseudo-first-order adsorption equation of MPP.

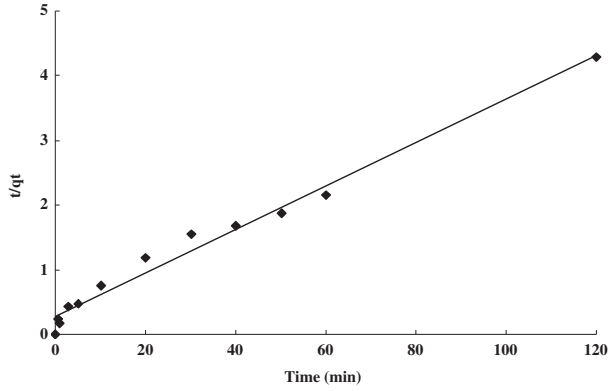

Fig. 8. Dynamic fitting results for the pseudo-second-order adsorption equation of MPP.

$$\frac{dq}{dt} = k_2(q_e - q_t)^2 \tag{6}$$

Here, k_2 is the pseudo-second-order rate constant (g adsorbent per g contaminant per min). The integration of Eq. (5) with the limit $q = 0$ at time $t = 0$ gives:

$$\frac{1}{q_e - q_t} - \frac{1}{q_e} = -k_2 t \tag{7}$$

Rearrangement of the above equation yields:

$$\frac{t}{q_t} = \frac{t}{q_e} + \frac{1}{k_2 q_e^2} \tag{8}$$

Therefore, a plot of (t/q_t) vs. time yields a straight line with the slope of $(1/q_e)$ and the y-intercept of $(k_2 {q_e}^2)^{-1}$. In this case, the results of dynamic equation are fitted with the pseudo-second-order equation of adsorption (Fig. 8). Parameter values obtained for all cases along with the goodness of fit, R^2 for diesel are summarized in Table 1. The result reveals that MPP (27.98 g/g) is efficient sorbent for oil spill recovery and is apparently superior than fatty acid-grafted banana trunk fibers (9.58–10.78 g/g) [26].

3.3. Equilibrium modeling

The isotherm data are obtained by diesel concentration measurement after sorbent/adsorbate contact periods equal to the equilibrium time. Out of several isotherm equations developed to describe the adsorption isotherm relationships, two models were applied for the equilibrium data of MPP: Langmuir and Freundlich isotherms. Langmuir adsorption model [27] assumes that adsorption occurs at specific homogeneous adsorption sites within the adsorbent and intermolecular forces decrease rapidly with the distance from the adsorption surface. The model further based on the assumption that all the adsorption sites are energetically identical and adsorption occurs on a structurally homogeneous adsorbent. Langmuir model which has been successfully applied to many sorption processes is

$$Q_e = \frac{Q_0 b C_e}{1 + b C_e} \tag{9}$$

The linear form of Langmuir isotherm is expressed as

$$\frac{1}{Q_e} = \frac{1}{Q_0} + \frac{1}{b Q_0 C_e} \tag{10}$$

Table 1
Comparison of the pseudo-first-order, pseudo-second-order sorption rate constants and calculated q_e values

Order	R^2	q_e (g/g)	K (min^{-1})	Slope	Intercept
Pseudo-first order	0.8370	26.58	0.0655	−0.0655	3.2800
Pseudo-second order	0.9823	29.76	0.0040	0.0336	0.2826

wherein Q_e is amount of diesel sorbed at equilibrium per unit mass of sorbent (mg/g) and C_e is the equilibrium concentration of diesel in solution (mg/L). The constant Q_0 signifies the maximum sorption capacity (mg/g) and b is related with the energy of the adsorption (L/mg). A plot of $1/Q_e$ vs. $1/C_e$ (Fig. 9) yields a straight line with slope $1/bQ_0$ and intercept $1/Q_0$. The essential characteristics of Langmuir isotherm can be expressed in terms of a dimensionless constant separation factor R_L that is given by Eq. (11) [28]:

$$R_L = \frac{1}{1 + bC_0} \tag{11}$$

where in C_0 is the highest initial concentration of sorbate (mg/L), and b (L/mg) is the Langmuir constant. The value of R_L indicates the type of the isotherm to be either unfavorable ($R_L > 1$), linear ($R_L = 1$), favorable ($0 < R_L < 1$), or irreversible ($R_L = 0$). The value of R_L for adsorption of diesel onto MPP was 0.60–0.64. This value showed that the sorption behavior of MPP was favorable for the diesel ($R_L < 1$).

The Freundlich isotherm is an empirical equation employed to describe heterogeneous systems. The Freundlich equation is expressed as

$$Q_e = K_F C_e^{\frac{1}{n}} \tag{12}$$

where in K_F and n are the Freundlich constants with n giving an indication of how favorable the adsorption process is. The magnitude of the exponent, $1/n$, gives an indication of the favorability of adsorption. Values of $n > 1$ represent favorable adsorption condition [29]. Eq. (11) may be written in the logarithmic form as

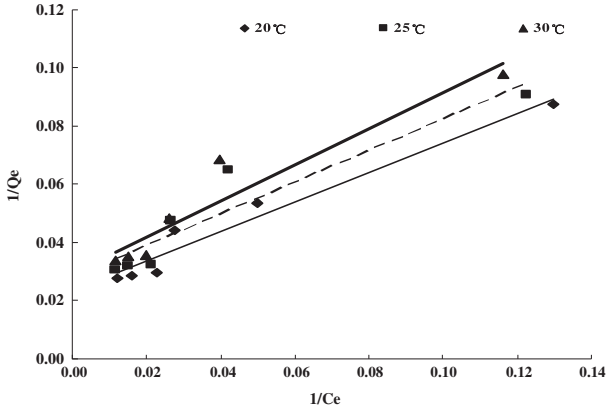

Fig. 9. Langmuir isotherm for diesel sorption onto MPP.

$$\ln Q_e = \ln K_F + \frac{1}{n} \ln C_e \tag{13}$$

The isotherm constants for all the isotherms studied, and the correlation coefficient, R^2, with the experimental data are listed in Fig. 10 and Table 2. In view of the values of linear regression coefficients and the oil sorption capacity in Table 2, Freundlich model exhibited better fit to the sorption data of MPP than Langmuir models and in the studied initial concentration range.

3.4. Effect of sorbent dosage

As can be seen from Fig. 11, the oil sorption capacity declines when the dosage of MPP is in the range from 0.01 to 0.09 g. The result is consistent with pervious result [30]. At certain oil amounts, increased sorbent dosage decreases sorption capacity per unit of sorbent, which can be attributed to possible sorbent aggregation. As the sorbent aggregates, total surface area decreases, diffusional holes are blocked and sorption site is unsaturated [31]. Therefore, in the subsequent reaction, the sorbent dose is fixed at 0.01 g.

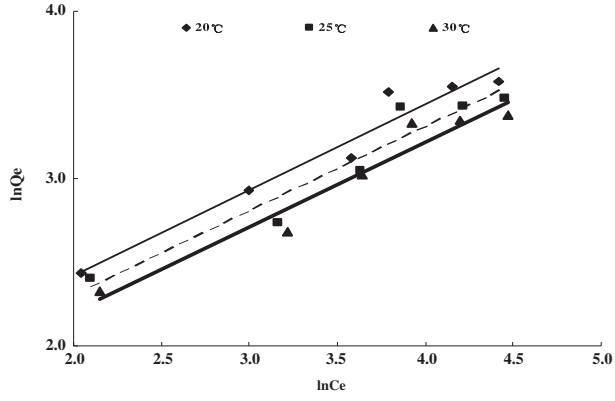

Fig. 10. Freundlich isotherm for diesel sorption onto MPP.

Table 2
Langmuir and Freundlich model constants and correlation coefficients for sorption of MPP on diesel

T (℃)	Freundlich			Langmuir		
	R^2	n	K_F	R^2	Q_0	b
20	0.9496	1.9550	4.0584	0.9600	42.74	0.5070
25	0.9275	1.9826	3.6223	0.8912	35.34	0.5394
30	0.9451	1.9790	3.3026	0.9143	33.56	0.6175

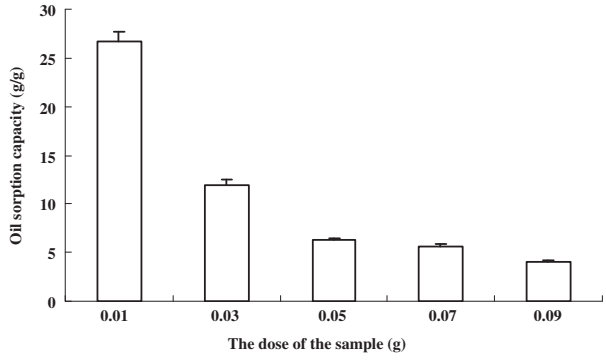

Fig. 11. The effect of the dose of sample on oil sorption capacity of MPP.

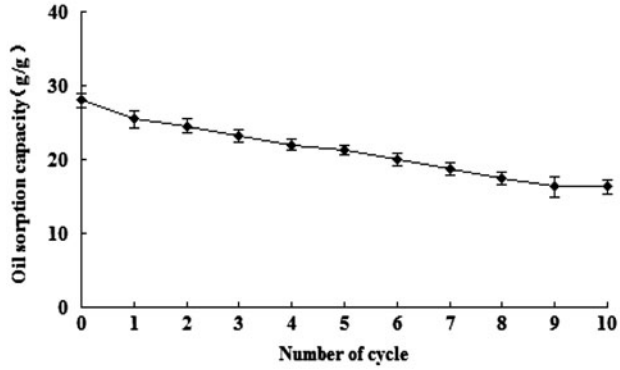

Fig. 13. The oil sorption capacity of MPP after different cycles.

3.5. Effect of oil amounts

Fig. 12 shows the oil sorption capacity of MPP at different temperature and different oil amounts. The overall trend is that the oil sorption capacity of MPP gradually increases with the rising oil amounts. The highest sorption capacity of MPP is at an initial oil amount of 1.50 mL. Sokker et al. [32] found that more oil molecules adhere to sorbent surface at a higher initial oil amount, which enhanced oil diffusion. As the oil film thickness increased, the oil sorption capacity of corn stalk increased [33].

Moreover, the oil sorption capacity of MPP increased in the order of 30℃ < 25℃ < 20℃. The reason might be that the oil sorption process of MPP was exothermic, and higher temperature was not conducive to the diesel sorption. Some researchers [34,35] found that when the temperature rose, the hydrophobicity of diesel was abated, and the solubility of diesel molecules in water increased, which made diesel harder to be absorbed from water. In addition, with the temperature rising, the viscosity of diesel reduced, the liquidity of diesel increased, and the Brownian motion of diesel particle accelerated, which could promote diesel particles and the adsorbent to collide with each other. On the other hand, it could also be the case that the diesel particle moved too fast and reduced the chances that was adsorbed, then reduced the diesel adsorption quantity.

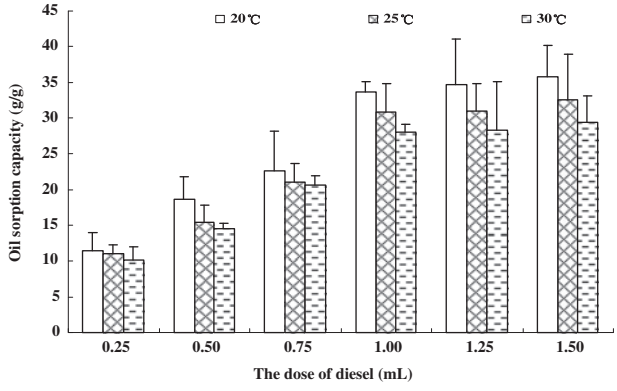

Fig. 12. The effect of diesel dose on oil sorption capacity of MPP.

3.6. Reusability

The sorbed MPP was reused in several sorption–desorption cycles to ascertain the efficiency. The quantities of oil sorbed were determined at the termination of each cycle for ten repeated cycles. As data shown in Fig. 13, the oil sorption capacity of MPP declined by 41.82% for diesel after 10 cycles. Moriwaki et al. [36] found that the oil sorption capacity of silkworm cocoon waste decreased after repeating the sorption treatment, might be due to the reduction of the specific surface area because of the aggregation of the oil between the fibers. Moreover, Likon et al. [37] found that extraction in hexane did not considerably affect the chemical composition and stability of the populus seed fibers. Therefore, the result indicates that the rejuvenated MPP is also able to retain its most original efficiency to sorb oil during ten repeated cycles, MPP can be reused numerous times for oil spill cleanup with the aid of n-hexane extraction.

4. Conclusions

This present work showed that MPP was successfully prepared by the solvothermal method. The sorption kinetics of MPP was well described by the pseudo-second-order kinetic model equation. Sorption of diesel onto MPP followed Langmuir isotherm model. The adsorption capacity of MPP was 27.98 g/g

for diesel. This novel oil sorbent could realize a facile, fast and highly efficient collection of oil in aqueous environments by means of an external magnetic field, so it was expected to replace traditional oil adsorption material for the large-scale cleanup of spilled oil from water surface.

Acknowledgments

The work was funded by the National Natural Science Foundation of China (Nos. 41373097, 41073072), China Postdoctoral Science Foundation funded project (No. 2013M541506), Program for Innovative Research Team in University (No. IRT13078).

References

[1] A.A. Al-Majed, A.R. Adebayo, M.E. Hossain, A sustainable approach to controlling oil spills, J. Environ. Manag. 113 (2012) 213–227.
[2] G. Hayase, K. Kanamori, M. Fukuchi, H. Kaji, K. Nakanishi, Facile synthesis of marshmallow-like macroporous gels usable under harsh conditions for the separation of oil and water, Angew. Chem. Int. Ed. 52 (2013) 1986–1989.
[3] T. Dalton, D. Jin, Extent and frequency of vessel oil spills in US marine protected areas, Mar. Pollut. Bull. 60 (2010) 1939–1945.
[4] J.E. Turbeville, Ferromagnetic sorbents for oil spill recovery and control, Environ. Sci. Technol. 7 (1973) 433–438.
[5] G. Wang, Q. Sun, Y. Zhang, J. Fan, L. Ma, Sorption and regeneration of magnetic exfoliated graphite as a new sorbent for oil pollution, Desalination 263 (2010) 183–188.
[6] L.C.A. Oliveira, R.V.R.A. Rios, J.D. Fabris, V. Garg, K. Sapag, R.M. Lago, Activated carbon/iron oxide magnetic composites for the adsorption of contaminants in water, Carbon 40 (2002) 2177–2183.
[7] L.C.A. Oliveira, R.V.R.A. Rios, J.D. Fabris, K. Sapag, V.K. Garg, R.M. Lago, Clay-iron oxide magnetic composites for the adsorption of contaminants in water, Appl. Clay Sci. 22 (2003) 169–177.
[8] H.H. Murray, Traditional and new applications for kaolin, smectite, and palygorskite: A general overview, Appl. Clay Sci. 17 (2000) 207–221.
[9] I.K. Konstantinou, T.A. Albanis, D.E. Petrakis, P.J. Pomonis, Removal of herbicides from aqueous solutions by adsorption on Al-pillared clays, Fe–Al pillared clays and mesoporous alumina aluminum phosphates, Water Res. 34 (2000) 3123–3136.
[10] Z.H. Sun, L.F. Wang, P.P. Liu, S.C. Wang, B. Sun, D.Z. Jiang, F.S. Xiao, Magnetically motive porous sphere composite and its excellent properties for the removal of pollutants in water by adsorption and desorption cycles, Adv. Mater. 18 (2006) 1968–1971.
[11] Q. Zhu, F. Tao, Q. Pan, Fast and selective removal of oils from water surface via highly hydrophobic core−shell Fe_2O_3@C nanoparticles under magnetic field, ACS Appl. Mater. Inter. 2 (2010) 3141–3146.
[12] G.L. Wang, Q.R. Sun, Y.Q. Zhang, J.H. Fan, L.M. Ma, Sorption and regeneration of magnetic exfoliated graphite as a new sorbent for oil pollution, Desalination 263 (2010) 183–188.
[13] C. Paola, F. Despina, S.B. IIker, C.A. George, M. Luigi, P.D. Cozzoli, C. Roberto, A. Athanassia, Magnetically driven floating foams for the removal of oil contaminants from water, ACS Nano 6 (2012) 5413–5419.
[14] Y. Zhou, C.W. Hu, C. Li, J.L. Li, H. Zhou, J.S. Huang, Physico-chemical characteristics of pomelo peel Adsorbent, Environ. Sci. Technol. 33 (2010) 87–91 (in Chinese).
[15] B.H. Hameed, D.K. Mahmoud, A.L. Ahmad, Sorption of basic dye from aqueous solution by pomelo (*Citrus grandis*) peel in a batch system, Colloid Surf. A 316 (2008) 78–84.
[16] L. Zhang, R. He, H.C. Gu, Oleic acid coating on the monodisperse magnetite nanoparticles, Appl. Surf. Sci. 253 (2006) 2611–2617.
[17] R.M. Cornell, U. Schwertmann, The Iron Oxides, VCH, New York, NY, 1996, p. 117.
[18] K. Woo, J. Hong, J.P. Ahn, Synthesis and surface modification of hydrophobic magnetite to processible magnetite@silica-propylamine, J. Magn. Magn. Mater. 293 (2005) 177–181.
[19] M. Ma, Y. Zhang, W. Yu, H.Y. Shen, H.Q. Zhang, N. Gu, Preparation and characterization of magnetite nanoparticles coated by amino silane, Colloids Surf. A 212 (2003) 219–226.
[20] Y.T. Tao, Structural comparison of self-assembled monolayers of n-alkanoic acids on the surfaces of silver, copper, and aluminum, J. Am. Chem. Soc. 115 (1993) 4350–4358.
[21] J.T. Wang, Y.A. Zheng, A.Q. Wang, Effect of kapok fiber treated with various solvents on oil absorbency, Ind. Crops Prod. 40 (2012) 178–184.
[22] C. Yin, X.Y. Wei, J.H. Li, F. Wang, Oleic acid surface modification effect on structure and dispersion of Fe_3O_4 nanoparticles, J. Magn. Mater. Dev 44 (2013) 24–27, 78 (in Chinese).
[23] Z.Y. Ma, Y.P. Guan, X.Q. Liu, H.H. Liu, Synthesis of magnetic chelator for high-capacity immobilized metal affinity adsorption of protein by cerium initiated graft polymerization, Langmuir 21 (2005) 6987–6994.
[24] S. Mørup, Magnetic hyperfine splitting in mössbauer spectra of microcrystals, J. Magn. Magn. Mater. 37 (1983) 39–50.
[25] D. Mysore, T. Viraraghavan, Y.C. JIN, Treatment of oily waters using vermiculite, Water Res. 39 (2005) 2643–2653.
[26] K. Sathasivam, M.R.H. Mas Haris, Adsorption kinetics and capacity of fatty acid-modified banana trunk fibers for oil in water, Water Air Soil Pollut. 213 (2010) 413–423.
[27] I. Langmuir, The adsorption of gases on plane surfaces of glass, mica and platinum, J. Am. Chem. Soc. 40 (1918) 1361–1403.
[28] K.R. Hall, L.C. Eagleton, A. Acrivos, T. Vermeulen, Pore- and solid-diffusion kinetics in fixed-bed adsorption under constant-pattern conditions, Ind. Eng. Chem. Fundamen. 5 (1966) 212–223.
[29] Y.S. Ho, G. McKay, Sorption of dye from aqueous solution by peat, Chem. Eng. J. 70 (1998) 115–124.

[30] D. Peng, Z.L. Lan, C.L. Guo, C. Yang, Z. Dang, Application of cellulase for the modification of corn stalk: Leading to oil sorption, Bioresour. Technol. 137 (2013) 414–418.
[31] S.M. Sidik, A.A. Jalil, S. Triwahyono, S.H. Adam, M.A.H. Satar, B.H. Hameed, Modified oil palm leaves adsorbent with enhanced hydrophobicity for crude oil removal, Chem. Eng. J. 203 (2012) 9–18.
[32] H.H. Sokker, N.M. El-Sawy, M.A. Hassan, B.E. El-Anadouli, Adsorption of crude oil from aqueous solution by hydrogel of chitosan based polyacrylamide prepared by radiation induced graft polymerization, J. Hazard. Mater. 190 (2011) 359–365.
[33] M.M. Li, H.C. Pan, S.L. Huang, M. Scholz, Controlled experimental study on removing diesel oil spillages using agricultural waste products, Chem. Eng. Technol. 36 (2013) 673–680.
[34] Y. Xie, Z. Huang, X. Wang, L. Wang, An experimental study of petroleum pollutant's adsorption and release from river sediments, Environ. Eng. 18 (2000) 58–60 (in Chinese).
[35] X.K. Zhao, G.P. Yang, X.C. Gao, Studies on the sorption behaviors of nitrobenzene on marine sediments, Chemosphere 52 (2003) 917–925.
[36] H. Moriwaki, S. Kitajima, M. Kurashima, A. Hagiwara, K. Haraguchi, K. Shirai, R. Kanekatsu, K. Kiguchi, Utilization of silkworm cocoon waste as a sorbent for the removal of oil from water, J. Hazard. Mater. 165 (2009) 266–270.
[37] M. Likon, M. Remškar, V. Ducman, F. Švegl, Populus seed fibers as a natural source for production of oil super absorbents, J. Environ. Manage. 114 (2013) 158–167.